RESEARCH PAPER

Effect of Collars on the Downstream Movement of the Maximum Scour Depth Location Around Bridge Abutments and Piers

Serife Yurdagul Kumcu[1] · Mehmet Ali Kokpinar[2] · Mustafa Gogus[3]

Abstract

A detailed investigation has been conducted to study the shift location of the point of the maximum scour depth for both bridge abutment-collar and pier-collar arrangements. In the present study, an experimental program has been conducted for abutment-collar arrangements and additionally, the data obtained from the literature for the pier-collar arrangements have been revisited and analyzed to complement the framework of this study. For the abutment-collar arrangements, a series of experiments under clear-water conditions were carried out for different abutment lengths with fixed values of collar location and collar width. For pier-collar arrangements, data used from the literature have been involved constant pier diameter with various collar sizes at various elevations. To describe the locations of these maximum scour depths, their coordinates with respect to the location of the abutment or the pier were obtained. Results from this investigation showed that when a collar placed on or below the bed level was used as a countermeasure against scouring, either on an abutment or on a pier, it was observed that the maximum scour depth was routed downstream of the bridge structure.

Abbreviations

B	Width of the channel
B_a	Width of the abutment
B_c	Width of the collar
d_{50}	Median grain size of the sediment
d_{84}	Sediment sizes for which 84% of the sediments are finer
d_{16}	Sediment sizes for which 16% of the sediments are finer
Fr	Froude number
g	Gravitational acceleration
L	Shift distance of the maximum scour depth location around bridge abutment or pier with a collar
L_a	The length of the abutment perpendicular to the flow direction
Re	Reynolds number
S	Slope of the channel
t	Time of scour
T_c	Thickness of the collar
U	Mean velocity of the approach flow
U_c	Critical velocity for initiation of sediment particle motion
x	Coordinate system axis
y	Depth of the approach flow
Z_c	Elevation of the collar with respect to the bed level
$Ź$	Coordinate system axis
σ_g	Geometric standard deviation of sediment size distribution, $(d_{84}, d_{16})^{0.5}$
θ	Angle of maximum scour depth deviation (in degree)
ρ_s	Density of the sediment
ρ	Density of the fluid
μ	Dynamic viscosity of the fluid

✉ Mehmet Ali Kokpinar
 mehmet.kokpinar@tedu.edu.tr

 Serife Yurdagul Kumcu
 yurdagulkumcu@gmail.com

 Mustafa Gogus
 mgogus@cankaya.edu.tr

[1] Civil Engineering Department, Necmettin Erbakan University, Hydraulic Division, Konya, Turkey

[2] Civil Engineering Department, TED University, Ankara, Turkey

[3] Civil Engineering Department, Çankaya University, Ankara, Turkey

Springer

1 Introduction

Scouring can lead to the main failure of bridge structures during flood events in rivers. Among these failures, scour around abutments and piers have been recognized as the cause of many cases. Despite its high importance, prediction of scour around bridge abutments has been known to be particularly difficult because of the complex system of factors causing the failure. Although a large part of the previous research was on the prediction of maximum scour depth and flow mechanisms causing scour, the location of the scour hole with respect to bridge structures draws less attention. Nevertheless, the knowledge of scour hole location may help taking measures on the failure risk of the bridge and surrounding structures. Downstream movement of scour hole was reported in several previous studies as explained below.

Kuhnle et al. (1999) studied the geometry of scour holes associated with 90° spur dikes on a 30 m long test channel using a median size of sediment particles of $d_{50} = 0.8$ mm. Two spur dike lengths of 0.305 m and 0.152 m were used in the study. It was interpreted that the region of the maximum scour shifts toward the channel bank and causes a secondary scour zone downstream of the spur dike. Kas (2005) experimentally investigated scour protection around bridge piers by using collars in a test channel of 1-m wide and 30-m long. Uniform sediment size of $d_{50} = 1.775$ mm was used as bed material. During experiments, the diameter of the bridge pier was kept constant as $d = 0.1$ m, while circular-shaped collars of diameters were varied as $D = 0.20$, 0.25, and 0.30 m. Other than circular collars, semi-circular and elliptical forms of collars were also used in the experimental campaign. In the study of Kas (2005), collars affixed on bridge piers $Z_c/y = +0.2$, 0, -0.2 (where $Z_c =$ location of the collar on the pier and $y =$ upstream approach flow depth) were investigated by conducting tests to determine the effects of flow conditions, the shape of the collar, and vertical position on the scour process around the bridge pier. The deviation in the location of the maximum scour depths were also measured when a collar located at $Z_c/y = -0.20$ was used on bridge piers. The measurements showed that the region of the maximum scour was moved downstream at a distance of approximately 1.8d and with an angle of deviation $23°- 53.4°$ from the center of the pier. Data obtained from Kas (2005) were revisited and analyzed in the present study.

Abutment scour in compound channels was experimentally studied by Sturm (2006) using different compound channel geometries by taking into account the flow redistribution that occurs between the floodplain and the main channel in the contracted section created by the bridge opening. For the setback vertical-wall abutments, it was pointed out that as discharge increases the maximum scour depth moves from the face of the abutment to an adjacent point near the abutment. Sturm observed similar behavior for the spill-through abutments as well. According to Sadat and Tominaga (2013), in the case of spur dike without a footing, the scour hole is generated around the spur dike, and the maximum scouring depth is located at the tip of the spur dike. On the other hand, in the case of a spur dike with a footing, the scour hole is shifted to the downstream of the spur dike in the main channel. Tests on different lengths of vertical-wall abutment-collar arrangements were conducted by Kumcu et al. (2013) and they predicted that the presence of a collar placed on an abutment deeper than bed level causes the movement of maximum scour depth location along the downstream direction away from the abutment. Hong and Abid (2019) investigated experimentally on erodible abutments located in a compound channel section. Observation of temporal development of the maximum scour depth was showed that the location of the deepest scour depth migrated over time from the upstream corner to a point that was diagonally displaced in the downstream direction from the abutment. Osroush et al. (2019) worked on the scouring around the abutments having various slots. They showed that slots can be used in order to reduce scour depth efficiently. Later on the this study, Osroush et al. (2021) examined the use of a slot or a collar, one by one or both together to reduce scour at bridge abutments. According to the results, collars were placed at the bed level and the experiments were illustrated that while collar length is increasing, the scour depth decreases and the scour hole shifts downstream farther away from the abutment. Other than the aforementioned studies given above, the application of collars to abutments as a scour countermeasure method has been investigated in detail by many researchers (Mohamed et al. 2015; Ettema et al. 2016; Nasr-Allah et al. 2016; Khosravinia et al. 2018; Karami et al. 2018).

Since abutment-collar or pier-collar arrangements can be an appropriate protection alternative as seen in Fig. 1, all analyses performed in the present study were based on the application of the collar protection to scour around abutments and piers. Literature research has shown that the work done with collars in the past has mainly studied the amount of maximum scour depth. On the other hand, studies on the location of the maximum scour depth have not been made conceptually and analyzed in depth. This study, therefore, was intended to investigate the downstream movement of the location of the maximum scour depth around an abutment-collar and a pier-collar arrangement of different geometrical characteristics and flow conditions.
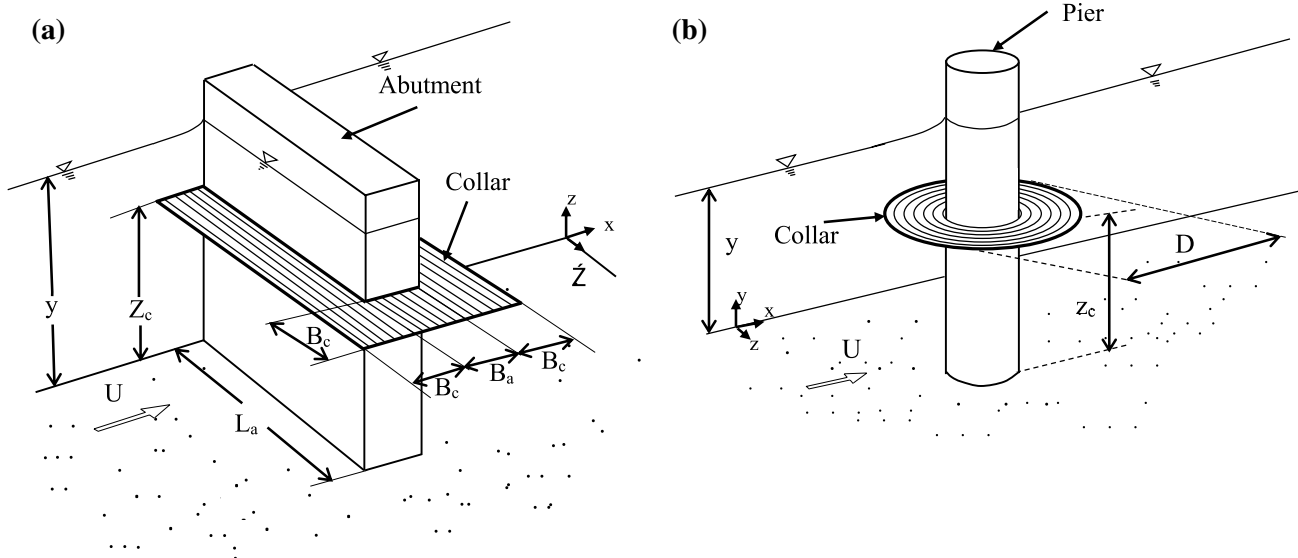
Fig. 1 Definition sketch of a typical **a** abutment-collar, **b** pier-collar arrangements in a channel flow

2 Dimensional Framework

2.1 Abutment-collar Arrangement

Referring to Fig. 2a, relevant parameters affecting shift distance L of the maximum scour depth location around bridge abutment with a collar may be related to; average approach flow velocity U, location of the collar relative to the channel bed level Z_c, abutment length L_a, approach flow depth y, abutment width B_a, collar width B_c, deviation angle of the maximum scour depth θ channel width B, channel bed material median size in which 50% of the bed material is finer d_{50}, sediment and the fluid densities,ρ_s and ρ, respectively, dynamic viscosity of the fluid μ, gravitational acceleration g, collar thickness T_c, channel bottom slope S, standard deviation of sediment size distribution $\sigma_g = (d_{84}/d_{16})^{0.5}$, and time t as given below:

$$L = f\left(U, Z_c, y, L_a, B_a, B_c, \theta, B, d_{50}, \rho_s, \rho, \mu, g, T_c, S, \sigma_g, t\right) \tag{1}$$

Equation (1) can be written in dimensionless form as,

$$\frac{L}{y} = f\left(\frac{U}{\sqrt{gy}}, \frac{Z_c}{y}, \frac{L_a}{y}, \frac{B}{y}, \frac{B_a}{y}, \frac{B_c}{y}, \frac{T_c}{y}, \theta, \frac{\rho_s}{\rho}, \frac{\mu}{Uy\rho}, \frac{Ut}{y}, S, \sigma_g, \frac{d_{50}}{y}\right) \tag{2}$$

One can replace (B/y), (L_a/y), (B_a/y), and (B_c/y) with (L_a/B) and (L_a/B_c) due to the purpose of the analysis since the empirical data are collected under steady clear-water flow conditions with constant values of S, B, L_a, T_c, σ_g, ρ_s, ρ, Z_c. Moreover, considering the only end scour depth at

the end of the test period instead of its temporal variation, then the dimensionless parameter including time t can be removed from Eq. (2) as:

$$\frac{L}{y} = f\left(Fr, Re, \frac{L_a}{B}, \frac{L_a}{B_c}, \theta, \frac{d_{50}}{y}\right) \tag{3}$$

where Fr and Re are the Froude and Reynolds numbers which are defined as $\frac{U}{\sqrt{gy}}$ and $\frac{Uy\rho}{\mu}$, respectively. Nevertheless, the flow in the channel is fully turbulent under the test conditions, one can, therefore, neglect the effect of Reynolds number. Besides, one may also replace Fr and d_{50}/y with a single non-dimensional parameter of flow intensity U/U_c which represents both flow and sediment size effects, where U_c is the critical velocity for initiation of sediment particle motion. Then, the final form of the functional relationship of the dimensionless terms can be written as;

$$\frac{L}{y} = f\left(\frac{L_a}{B}, \frac{L_a}{B_c}, \theta, \frac{U}{U_c}\right) \tag{4}$$

2.2 Pier-collar Arrangement

en a similar dimensional analysis is performed for a pier-collar arrangement as shown in Fig. 2b, then the resulting dimensionless relationship can be written as;

$$\frac{L}{y} = f\left(\frac{d}{D}, \theta, \frac{Z_c}{y}, \frac{U}{U_c}\right) \tag{5}$$

in which d and D are the pier and collar diameters, respectively. In Eq. (5), on the contrary to Eq. (4), Z_c/y effect is also considered

Fig. 2 Definition sketches of θ and L in the plan view for **a** bridge abutments, and **b** bridge piers
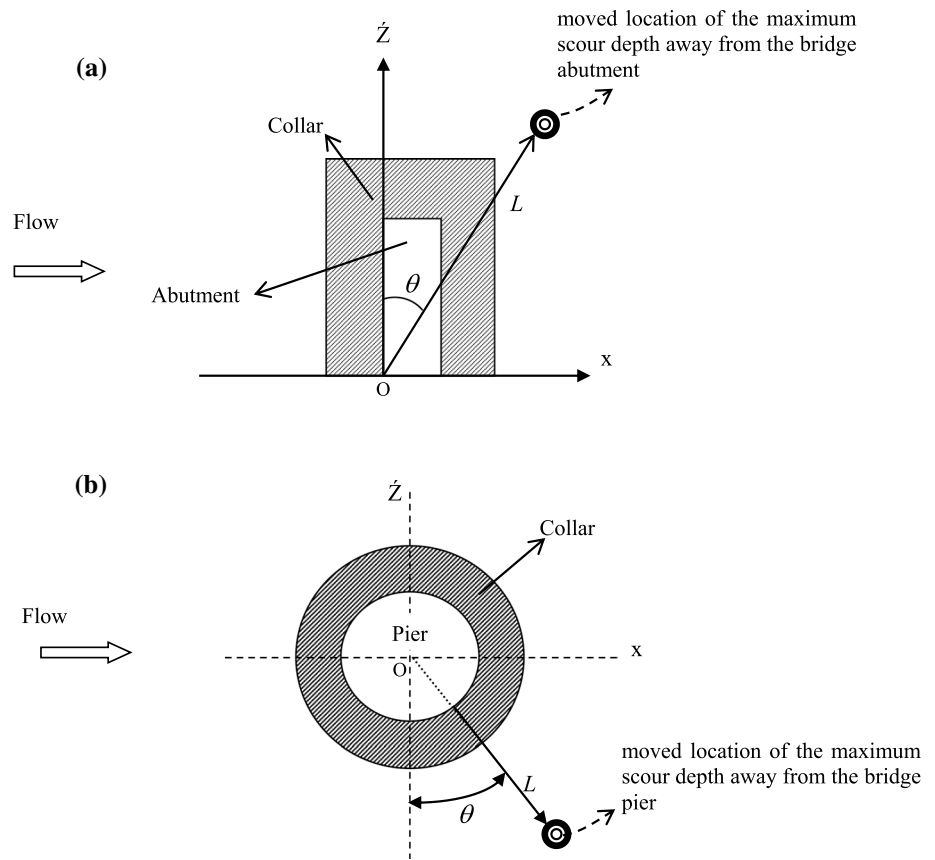
with cases of $Z_c/y = 0$ and —0.2 which are available for experimental data obtained from Kas (2005). However, only one pier diameter $d = 0.1$ m and constant channel width of $B = 1.0$ m were used in the experiments, then the effect of the d/B ratio is neglected.

3 Experiments

Experimental tests for abutments were conducted at the Hydraulics Laboratory of State Hydraulic Works of Turkey (DSI) in a 30 m long and 1.5 m wide channel with erodible bed material having a uniform median sediment size of $(d_{50}) = 1.48$ mm and standard deviation of the size distribution of $\sigma_g = 1.28$. For all cases, the test duration was set to a 12 h continuous run under clear-water flow conditions. The bottom slope of the test channel was 0.001 and a recession basin containing sediment was formed 13 m from the channel inlet (Fig. 3). A comprehensive description of the experimental set-up and test procedure is also available in Kayaturk et al. (2004a; 2004b), Kumcu et al. (2007), and Kumcu et al. (2014).

During the experiments, effects of abutment lengths, L_a, and flow intensities, U/U_c, on the downstream movement of the maximum scour depth location were studied on

abutments with a collar placed at the most effective elevation against scouring of $Z_c/y = -0.5$ (Kayaturk et al. (2004a, b)). In other words, each collar was placed on the abutments at 0.05-m below the bed level for the objective of this study. Constant widths of collar ($B_c = 0.10$ m) and abutment ($B_a = 0.10$ m) were used with various lengths of abutments of $L_a = 0.15$, 0.20, and 0.25 m. Only a few tests were conducted qualitatively for smaller-sized collars of $B_c = 0.025$ and 0.05 m located above the bed level in order to make a comparison with collars at and below the bed level. Referring to the bed profiles measured at the end of each experiment, the location of maximum scour depth around the abutment was determined, and both shift distance and deviation angle were calculated. Experimental conditions of the present study and that conducted by Kas (2005) for circular piers are summarized in Table 1 and Table 2, respectively.

4 Discussion of Results

4.1 Abutment-collar Arrangement

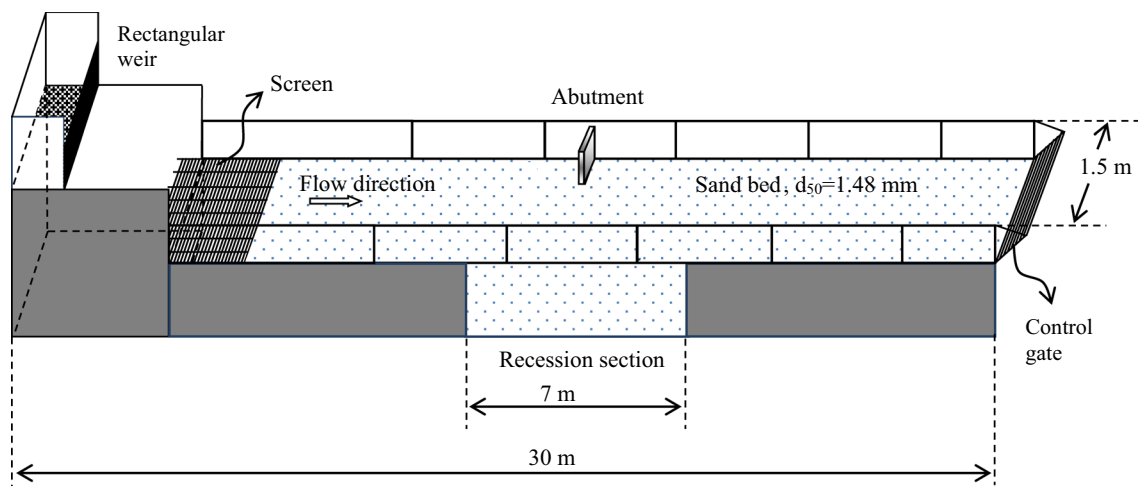If no protection measure is considered against scour development, the location of the maximum scour is observed at

Fig. 3 Experimental setup used in the experimental campaign

the upstream corner of an abutment (Melville 1992; Lim 1997; Melville and Coleman 2000; Kayaturk 2005; Garcia 2007; Osroush et al. 2021). The scour mechanism is initiated because of down flow at the upstream face of the abutment and the subsequent development of the principal vortex at the base. One way of reducing scour is to weaken and possibly prevent the formation of the downflow and the horseshoe vortex. In this manner, placing a collar on the abutment can make these vortex structures ineffective. A collar divides the flow into two regions; i.e., above and below the collar. For the region above the collar, it acts as an obstacle against the downflow in which the downflow loses its strength on impingement at the bed. For the region below the collar, the downflow and the principal vortex are reduced. The efficacy of a collar depends on its size and the location at the abutment with respect to the bed as well. Kumcu et al. (2014) recommended that collar location on or below the bed is more effective against scour.

Abutments having small-sized collars may behave similarly to the abutments with no collars and the location of the maximum scour depth may be unchanged and remains at the upstream corner of the abutment. In this respect, Fig. 4 indicates that a small-sized collar (i.e., $B_c = 0.050$ m) which is placed above the bed level, $Z_c/y = +0.50$, the location of the maximum scour depth is identical with the non-collar abutment cases. On the other hand, when large-sized collars (i.e., $B_c = 0.10$ m) are placed at lower elevations, such as $Z_c/y = -0.50$, the location of the maximum scour hole moved to a distance along the flow direction from the upstream corner of the abutment (see Figs. 5 and 6). It can be deduced that flow altering scour mitigation techniques, for example collars in this case, applied to an abutment may cause shifting of the maximum scour depth location to a region downstream of the abutment.

Table 1 presents the experimental conditions together with the data used in the analysis of the tested abutments. Although the shifted maximum scour depths, $(d_s)_{ac}$, are greater than those recorded at the abutment faces when there are collars, $(d_s)_{maxc}$, they are still less than the maximum scour depths obtained from the cases without collars, $(d_s)_{max}$ (see Table 1, columns (6), (7), and (8)). From Table 1, the averages of reduction in scour depth between cases of no-collar, $(d_s)_{max}$, and collar with shifted maximum scour depth, $(d_s)_{ac}$, can be calculated as 38.2, 27.3, and 25.1% for the abutment lengths of $L_a = 0.15$, 0.20, and 0.25 m, respectively. As shown in Table 1, the experiments for abutment-collar arrangements were conducted under the condition of a range of flow Froude numbers between $0.41 \leq Fr \leq 0.57$, collar placed below bed level, and constant collar dimensions. On the other hand, Osroush et al. (2021) stated that the average reduction rates in maximum shifted scour depth ranged from 49 to 56% under conditions where the flow Froude numbers varied from 0.28 to 0.36 when collars were placed at the bed level. The lower reduction rate in the present study is thought to be caused by the differences in the Froude numbers of the two studies. Compared with the previous study, in the present study, since experiments have been carried out under higher Froude numbers, the depth of scour has become normally higher. It should be kept in mind that other than the Froude number, another important effect is the sediment size differences between these two studies. It can be also inferred from the present conducted tests that longer abutments have less scour depth reduction rate when a collar is placed below bed level. The main reason for the maximum scour depth shifting along the downstream direction is the presence of the collar plate located at an elevation below the bed level. When scour depth reaches the collar elevation, then the collar plate alters the flow structure around

Table 1 Experimental data for the abutments in the present study ($B_c = 0.10$ m, $Z_c/y = -0.50$, $B = 1.5$ m)

L_a (cm) (1)	Q (l/s) (2)	U/U_c (3)	y (cm) (4)	Fr (5)	$(d_s)_{maxc}$ (cm) (6)	$(d_s)_{max}$ (cm) (7)	$(d_s)_{ac}$ (cm) (8)	$Ź$ (cm) (9)	X (cm) (10)	$\theta(°)$ (11)	L (cm) (12)	L/L_a (13)	L/y (14)
15	35	0.86	6.45	0.57	5	15.5	9.4	29.6	11	20.4	31.57	2.10	4.89
15	40	0.88	7.15	0.53	5	16.1	10.2	30.5	12.5	22.3	32.96	2.19	4.61
15	45	0.89	7.95	0.48	5	15.4	8.6	30	15.5	27.3	33.76	2.25	4.25
15	50	0.90	8.85	0.43	5	15.7	9	31	16	27.3	34.88	2.32	3.94
15	55	0.91	9.60	0.41	5	16.1	11.1	31.5	11.5	20.1	33.53	2.23	3.43
20	35	0.86	6.45	0.57	5	17.5	13	33.5	20	30.8	39.01	1.95	6.05
20	40	0.88	7.15	0.53	5	17.5	13.5	33	21	32.5	39.11	1.95	5.47
20	45	0.89	7.95	0.48	5	18	13.5	36.5	19.5	28.1	41.38	2.06	5.21
20	50	0.90	8.85	0.43	5	18.2	13	35	22	32.1	41.34	2.07	4.67
20	55	0.91	9.60	0.41	5	18.6	13.4	35	21.6	31.7	41.13	2.05	4.28
25	35	0.86	6.45	0.57	5	18.1	15.1	44	30	34.3	53.25	2.13	8.26
25	40	0.88	7.15	0.48	5	19.4	15.5	48	31	32.9	57.14	2.28	7.99
25	45	0.89	7.95	0.48	5	20.3	15.8	46.5	36.2	37.9	58.92	2.35	7.41
25	50	0.90	8.85	0.43	5	20.6	14.7	46.5	41	41.4	61.99	2.47	7.00
25	55	0.91	9.60	0.41	5	21.5	13.2	48.5	44.1	45.9	67.53	2.70	7.03

L_a abutment length; Q discharge; y depth of flow; $(d_s)_{maxc}$ depth of scour with collar; $(d_s)_{max}$ depth of scour without collar; $(d_s)_{ac}$ depth of scour away from abutment with collar; B channel width

Table 2 Experimental data obtained from Kas (2005) for the piers

d (cm) (1)	Q (l/s) (2)	U (m/s) (3)	y (cm) (4)	D (cm)(5)	U_c (m/s) (6)	U/U_c (7)	θ (°) (8)	L (cm) (9)	Z_c/y (10)
10	25	0.36	7.09	20	0.44	0.818	53.4	14.30	0
10	30	0.38	8.03	20	0.44	0.863	24.6	8.20	0
10	25	0.36	7.09	25	0.44	0.818	40.6	13.44	0
10	30	0.38	8.03	25	0.44	0.863	35.1	11.51	0
10	35	0.40	8.81	25	0.44	0.909	31.0	12.49	0
10	40	0.42	9.61	25	0.44	0.954	24.0	9.77	0
10	25	0.36	7.09	30	0.44	0.818	23.0	12.92	0
10	30	0.38	8.03	30	0.44	0.863	31.2	14.29	0
10	35	0.40	8.81	30	0.44	0.909	41.2	16.26	0
10	40	0.42	9.61	30	0.44	0.954	44.1	18.69	0
10	25	0.36	7.09	20	0.44	0.818	66.4	21.20	− 0.2
10	25	0.36	7.09	25	0.44	0.818	68.5	25.08	− 0.2
10	30	0.38	8.03	25	0.44	0.863	35.4	14.01	− 0.2
10	25	0.36	7.09	30	0.44	0.818	66.6	27.70	− 0.2
10	30	0.38	8.03	30	0.44	0.863	70.6	31.06	− 0.2
10	35	0.40	8.81	30	0.44	0.909	36.0	15.40	− 0.2
10	40	0.42	9.61	30	0.44	0.954	30.5	14.72	− 0.2

Fig. 4 Abutment-collar arrangement and scour hole ($L_a = 0.25$ m, $Z_c/y = +0.50$ $B_c = 0.05$ m)

(a) Downstream view   **(b)** Upstream view

Location of the maximum scour depth
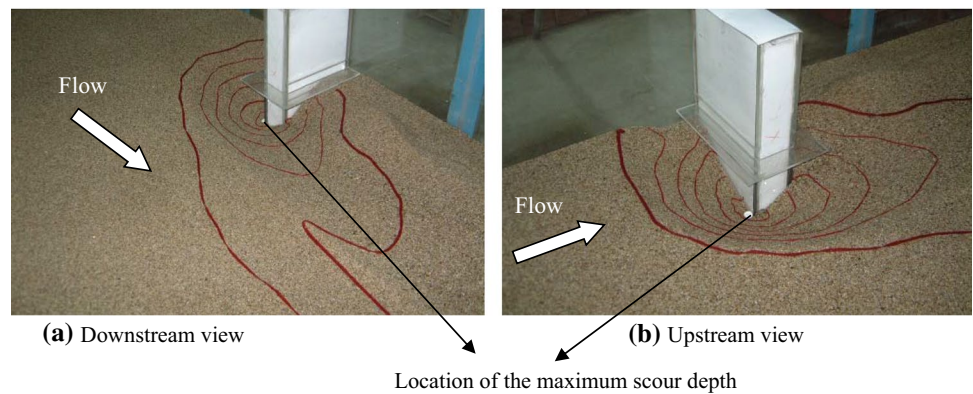
Fig. 5 Abutment-collar arrangement and scour hole ($L_a = 0.20$ m, $Z_c/y = − 0.5$, $B_c = 0.10$ m)

Location of the maximum scour depth

(a) Upstream view   **(b)** Top view
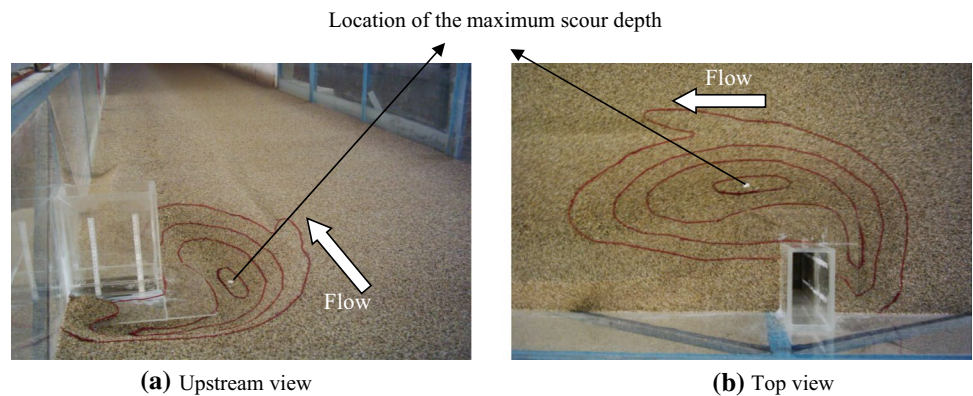
the abutment and reduces the strength of vortexes causing scour and changes their directions toward downstream. In other words, the main necklace vortex and horizontal vortex tubes generated from the abutment cause shifting of the location of the maximum scour depth around the bridge abutment, when a collar located below the bed level applied
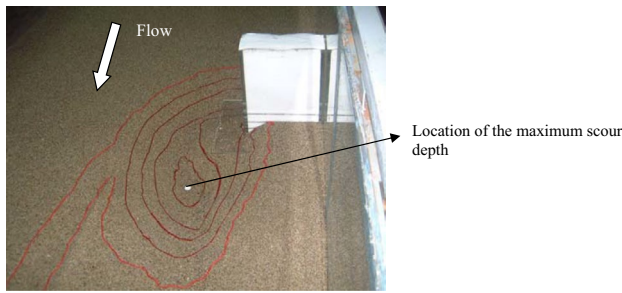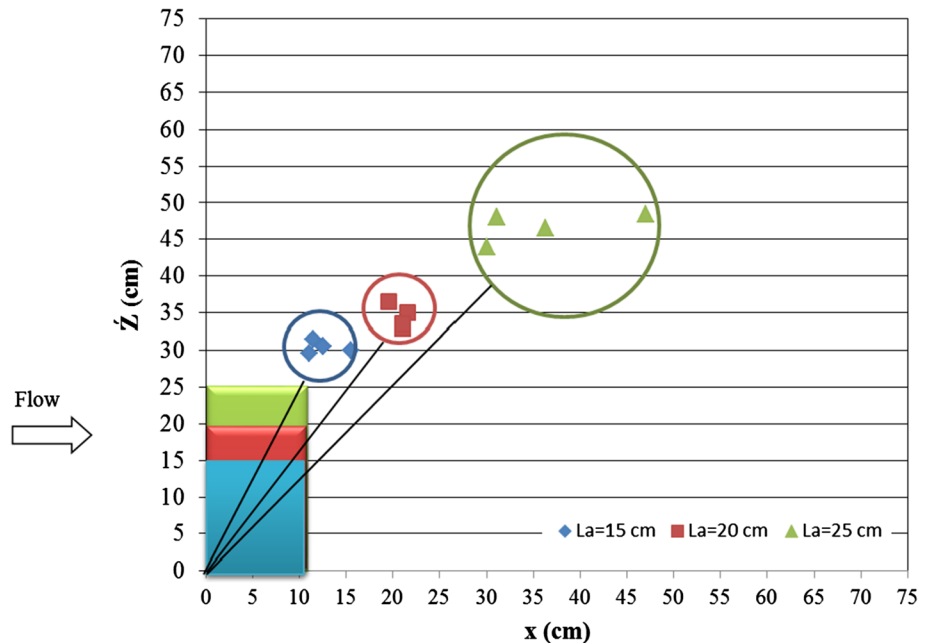
Fig. 6 View from downstream of the eroded bed around the abutment ($Q = 0.055$ m³/s, $y = 0.096$ m, $U/U_c = 0.91$, $L_a = 0.25$ m, $Z_c/y = -0.5$, $B_c = 0.10$ m)

for a countermeasure against scouring. Moreover, the ratio of shift distance to abutment length (L/L_a) values given in Table 1 (column 13) indicates that shifting of the maximum scour depth ranges between $1.95 \leq L/L_a \leq 2.70$ with giving an average value of $L/L_a = 2.3$ for all abutment lengths tested in the present study. Figure 7 is plotted in a supportively manner to comprehend distinguishing features of abutment length effect on shift distance. The regions showing the locations of the maximum shift distances are confined with circles in the x-$\acute{Z}$ coordinate system for various abutment lengths as seen in Fig. 7. The color of a circle is associated with the color of the corresponding abutment in this figure. Once again, it can be clearly seen that long abutments create longer shift distances and more diagonally spread of scour depth locations along with downstream directions. The relocation of the maximum scour depth is important in practice for the abutment stability considerations. Moreover,

another important point may be the existence of another bridge structure (pier or abutment) at the new location of the maximum scour depth which may create an additional scouring mechanism that should be also considered in the analysis and design.

Variation of non-dimensional shift distance, L/y, with abutment length to collar width ratio L_a/B_c as a function of flow contraction ratio L_a/B is shown in Fig. 8. Non-dimensional shift distance is directly proportional to both the increase in L_a/B_c ratio and flow contraction by abutment (L_a/B). The averaged values of L/y data for each of the three
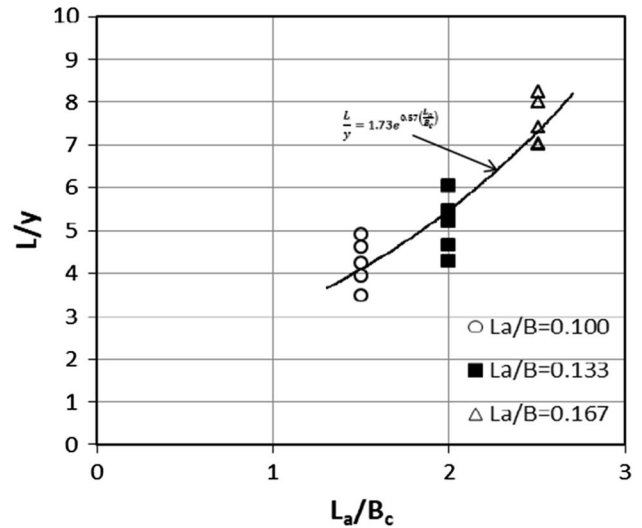

Fig. 8 Variation of L/y with L_a/B_C as a function of L_a/B

Fig. 7 Moved locations of the maximum scour depths and the corresponding θ and L values as a function of abutment length L_a (flow is from left to right)

tested abutment-collar arrangements appear to follow a simple exponential relationship as given in the figure. The trend line of this relationship is in the form of;

$$\frac{L}{y} = 1.73e^{0.57\left(\frac{L_a}{B_c}\right)} \tag{6}$$

Shift distance L can be calculated using Eq. (6) for the given flow depth, abutment length, and collar size. However, it should be kept in mind that Eq. (6) is valid only within the experimental conditions, flow contraction range of $0.100 \leq L_a/B \leq 0.167$, and especially sediment size used in the tests.

In order to geometrically describe the location of maximum scour depth for an abutment, the deviation (shift) angle θ and length L are defined according to the x-$\acute{Z}$ coordinate system as illustrated in Fig. 2a. Herein, the angle θ is measured between the axis, which coincides with the upstream face of the abutment perpendicular to the flow, and the line connecting the origin of the x-$\acute{Z}$ coordinate system to the point where the maximum scour depth measured (Fig. 2a). Figure 9 presents the relationship between non-dimensional shift distances L/y with the angle of the maximum scour depth deviation θ as a function of the L_a/B ratio. In general, it is seen that the deviation angle θ increases with decreasing L/y ratio for any channel contraction ratio L_a/B. This situation is similar for all three contraction ratios L_a/B. For example, for a constant value of $L_a/B = 0.167$, θ value for $L/y = 8.26$ is 34.3°, while for L/y = 7.03 θ increases to 44.1°. Likewise, when Fig. 9 is examined in terms of channel contraction effect, it is noteworthy that the angle of deviation increases with the increase in contraction ratio of L_a/B. It is seen that

the average deviation angle θ is 23.6°, 31.0°, and 37.9° according to the channel contraction ratios of $L_a/B = 0.100$, 0.133, and 0.167, respectively. In the experimental study of Osroush et al. (2021), if the channel contraction ratio is $L_a/B = 0.18$ and the L/y ratio is around 4, it was observed that the deflection angle is around 40° according to the coordinate system defined in this study. This shows that the results obtained in this study are also in accordance with the findings in the literature.

Effect of flow intensity U/U_c on non-dimensional shift distance L/y as a function of the L_a/B ratio is given in Fig. 10. The increase in flow intensity U/U_c inversely affects the non-dimensional shift distance L/y for a given channel contraction ratio L_a/B. This trend shows that the dimensionless shift length will reach a minimum value as the flow intensity approaches the threshold $U/U_c = 1$, provided the channel contraction is constant. The effect of channel contraction ratio on the shift distance is also seen in this figure under conditions of known flow intensity. Within this context, for the constant flow intensity value of U/U_c, the dimensionless shift length L/y increases with the increase in contraction ratio of L_a/B.

4.2 Pier-collar Arrangement

In the light of dimensional framework given by Eq. (5), the pier-collar arrangement data obtained from the experimental study of Kas (2005) were reanalyzed and interpreted in the present study. Table 2 summarizes the data used in the analysis with the definition of geometrical parameters as shown in Fig. 2b. At this point, it should be reminded that the data used were collected for a constant pier diameter but different
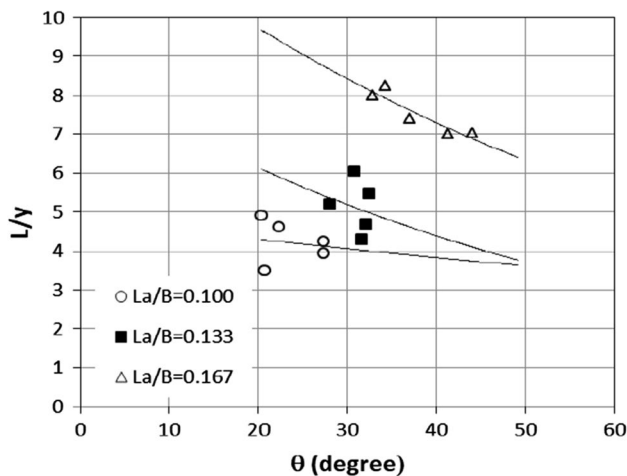

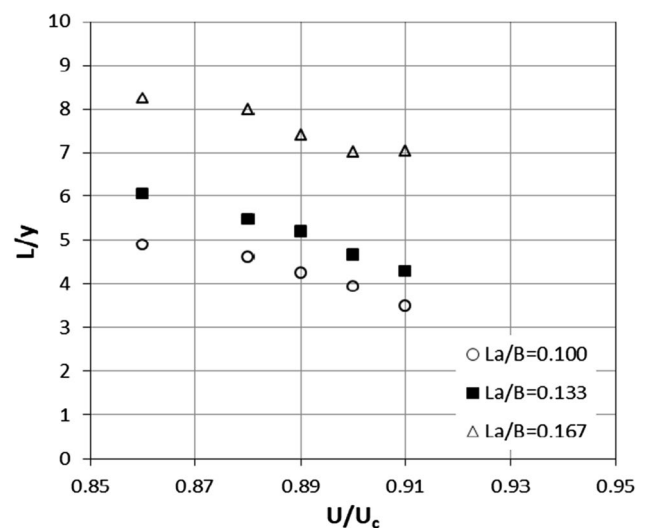**Fig. 9** Variation of L/y with θ as a function of L_a/B

Fig. 10 Variation of L/y with U/U_c as a function of L_a/B

collar diameters, collar elevations, and flow intensity values. In the previous discussion, on the other hand, the data used for the abutments were obtained at different abutment lengths and flow intensities by keeping the collar width and collar elevation level constant. For this reason, rather than directly comparing the situations in these two bridge structures with each other, the data analyze within themselves were made separately.

The effect of pier diameter to collar size ratio d/D on non-dimensional shift distance L/y as a function of collar elevation is shown in Fig. 11. It could be realized herein that increases in collar size for a constant pier diameter result in longer shift distances. For example, the value of dimensionless shift distance L/y for 30 cm collar diameter with d/D ratio of 0.33 is close to 4, whereas this value is 3 for the 20 cm collar diameter. This means that, the larger the collar diameter, the more it moves away from the place where the maximum scour depth is. This is because the large diameter collar reduces the effectiveness of the vortex structure around the pier, allowing the scour to occur further away from the pier. If the location of the collar on the pier is taken into account, it is seen from Fig. 11 that the maximum scour depth is farther away in the collars placed below the sand level. In other words, when compared to the cases of collars at $Z_c/y = 0$, shift distances, in general, are longer for collars placed below bed level at $Z_c/y = -0.2$.

The relationship between non-dimensional shift distance L/y and the deviation angle of the maximum scour depth location θ (as defined in Fig. 2b) as a function of collar position Z_c/y is shown in Fig. 12. Longer shift distances are observed together with large deviation angles especially for collar position at $Z_c/y = -0.2$. Deviation angles are generally higher for those cases at $Z_c/y = -0.2$. On the other hand, the majority of data fall between 20° and 40°, which indicates
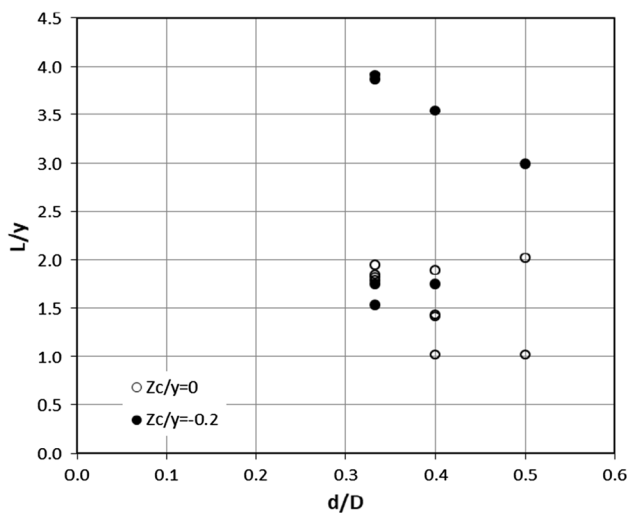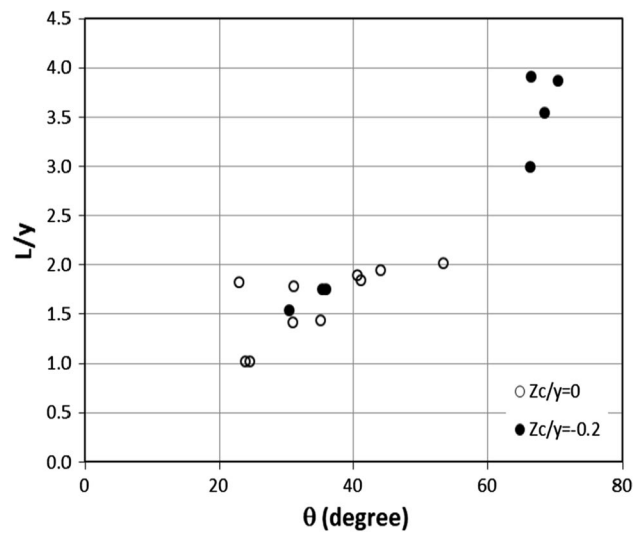
Fig. 12 Relationship between L/y and θ as a function of Z_c/y

that smaller shift angles and shift distances at the collar elevation of $Z_c/y = 0$.

Figure 13 illustrates the effect of flow intensity U/U_c on non-dimensional shift distance L/y as a function of Z_c/y ratio. Similar to the cases observed in abutment-collar arrangements, longer non-dimensional shift distances are observed in low flow intensity values for the piers. Shift distances take a value between 1.7 and 3.9 for $U/U_c = 0.818$ while for higher flow intensities like $U/U_c = 0.954$, this change is in a relatively small interval at 1.0 to 2.0. Also, it is clear from the Figure that if the collar location is below the bed level, the shift length increases when there is relatively low flow intensity.
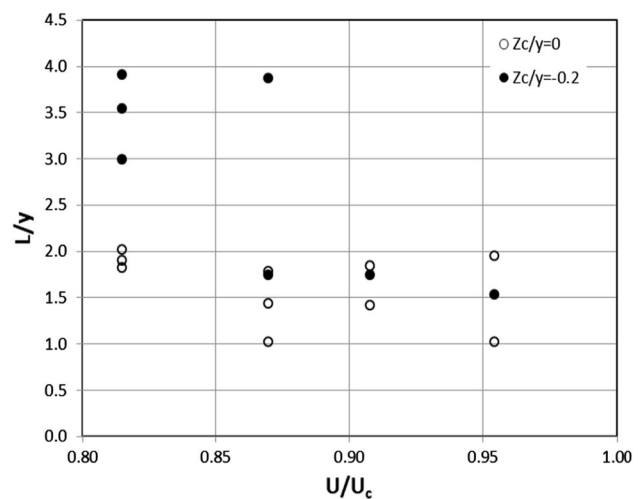
Fig. 11 Relationship between L/y and d/D as a function of Z_c/y

Fig. 13 Relationship between L/y and U/U_c as a function of Z_c/y

5 Conclusions

The effect of collars on the downstream shift of the maximum scour depth location was investigated for both abutment-collar and pier-collar arrangements. For this purpose, firstly an experimental study was conducted for abutment-collar arrangements using various lengths of abutments under different flow intensities while collar location and collar length were kept constant under the light of knowing the most effective values from the previous studies. Secondly, for the pier-collar arrangements, the data obtained from the study of Kas (2005) on pier-collar arrangements were re-analyzed. The following conclusions can be drawn from the results of experimental study:

1. The presence of a collar placed at or below bed level on an abutment or a pier causes movement of the maximum scour hole downstream direction away from the bridge structure. Moreover, the shifted maximum scour depth with a collar on the abutment is always less than that of the abutment having no collar case. Experimental studies have shown that decreased in the maximum-averaged scour depths are in the range between 25.1 and 38.2%.

2. Experiments on the abutment-collar arrangements have shown that when a collar placed above bed level has either limited or no effect on the shift of the maximum scour depth. Regarding the effect of flow intensity, the shift distance of the maximum scour depth decreases for both abutments and piers with the increase in U/U_c.

3. The deviation angle of the maximum scour depth increases with increasing the abutment length for abutment-collar arrangements. Flow contraction due to the L_d/B ratio seems to a positive effect on the increase in deviation angle. As to the pier-collar arrangements, analysis of data has been shown that deviation angle are directly proportional with the collar position on the pier. Collars placed on the pier deeper than the bed level cause an increase in deviation angle .

4. It should be noted that the analysis of results is limited to the range of test conditions. Further studies should focus on the sediment size effect for both piers and abutments by using various sand materials, different pier diameters, and also size of collars for abutments.

References

Chiew YM (1992) Scour protection at bridge pier. J Hydraulic Eng 18(9):1260–1269

Ettema RM, Bergendahl BS, Yorozuya A, Idil-Bektur P (2016) Breaching of bridge abutments and scour at exposed abutment columns. J. Hydraul. Eng. 142(10):06016010

Garcia MH (ed) (2007) Sedimentation engineering. ASCE Manuals and reports on engineering practice No: 110, Reston, Virginia

Hong SH, Abid I (2019) Scour around an erodible abutment with riprap apron over time. J Hydraulic Eng 145(6):060190071–060190076

Karami H, Hosseinjanzadeh H, Hosseini K, Ardeshir A (2018) Scour and three-dimensional flow field measurement around short vertical-wall abutment protected by collar. KSCE J Civil Eng 22(1):141–152

Kas I (2005) Effects of collars on local scour around bridge piers. Ph.D. thesis, Dept. of Civil Engineering, Gazi Univ., Ankara, Turkey (in Turkish)

Kayaturk S Y, Kokpinar, M A , Gogus, M (2004a). Reduction of local scour around bridge abutments with collars. In: Proc., 2nd Int. Conf. on Fluvial Hydraulics, Balkema, Napoli, Italy (pp. 609–614)

Kayaturk S Y, Kokpinar M A, Gogus, M (2004b). Effect of collar on temporal development of scour around bridge abutments. In: Proc., 2nd Int. Conf. on Scour and Erosion, Surbana, Meritus Mandarin, Singapore (pp. 180–186)

Kayaturk S Y (2005). Scour and scour protection at bridge abutments. Ph.D. thesis, Dept. of Civil Engineering, Middle East Technical Univ., Ankara, Turkey

Khosravinia P, Malekpour A, Hosseinzadehdalir A, Farsadizadeh D (2018) Effect of trapezoidal collars as a scour countermeasure around wing-wall abutments. Water Science and Engineering 11(1):53–60

Kuhnle RA, Alonso CV, Shields FD Jr (1999) Geometry of scour holes associated with 90° spur dikes. J Hydraulic Eng 125(9):972–978

Kumar V, Raju KGR, Vittal N (1999) Reduction of local scour around bridge piers using slots and collars. J Hydraulic Eng 125(12):1302–1305

Kumcu SY, Gogus M, Kokpinar MA (2007) Temporal scour development at bridge abutments with a collar. Can j Civ Eng 34(4):549–556

Kumcu SY, Gogus M, Kokpinar MA (2013). Effect of abutment-collar arrangement on the location of the maximum scour depth. In: Proceedings of 2013 IAHR Congress, Tsinghua University Press, Beijing.

Kumcu SY, Kokpinar MA, Gogus M (2014) Scour protection around vertical-wall bridge abutments with collars. KSCE J Civil Eng Korean Soc Civil Eng 18(6):1884–1895

Lim SY (1997) Equilibrium clear-water scour around an abutment. J Hydraulic Eng 123(3):237–243

Melville BW (1992) Local scour at bridge abutments. J Hydraulic Eng 118(4):615–631

Melville BW, Coleman SE (2000) Bridge scour. Water Resources Publications, LLC, Colorado, USA

Mohamed YA, Nasr-Allah TH, Abdel-Aal GM, Awad AS (2015) Investigating the effect of curved shape of bridge abutment provided with collar on local scour, experimentally and numerically. Ain Shams Eng J 6(2):403–411

Nasr-Allah TH, Moussa YAM, Abdel-Aal G, M, Awad, A S, (2016) Experimental and numerical simulation of scour at bridge abutment provided with different arrangements of collars. Alex Eng J 55(2):1455–1463

Osroush M, Hosseini SA, Kamanbedast AA, Khosrojerdi A (2019) The effects of height and vertical position of slot on the reduction of scour hole depth around bridge abutments. Ain Shams Eng J 10(3):651–659

Osroush M, Hosseini SA, Kamabedast AA (2021) Countermeasures against local scouring around bridge abutments: combined system of collar and slot. Iranian J Sci Technol Transac Civil Eng 45:11–25

Singh, C P, Setia, B, and Verma, D V S (2001). Collar-sleeve combination as a scour protection device around a circular pier. In: Proc. of 29th IAHR Congress, IAHR (pp. 202–210)

Sturm TW (2006) Scour around bankline and setback abutments in compound channels. J Hydraulic Eng 132(1):21–32

Sadat, S H and Tominaga, A (2013). Mitigation of local scour hazard at the foot of single spur dike by using optimum footin. In:

Proceedings of the 12th International Symposium On River Sedimentation, Advances in River Sediment Research, Taylor & Francis Group (pp. 869–878)

Zarrati AR, Gholami H, Mashahir MB (2004) Application of collar to control scouring around rectangular bridge piers. J Hydraulic Res 42(1):97–103